Small-Signal Characterization of a Forward Converter with Active Clamping and Complete Rectification of the Output Voltage

Günter Johann Maass, Alexandre Ferrari de Souza and Ivo Barbi

Power Electronics Institute - INEP
Dept. of Electrical Engineering
Federal University of Santa Catarina - UFSC
P.O. Box 5119 - 88040-970 - Florianópolis - SC -Brazil
alex@inep.ufsc.br - http://www.inep.ufsc.br

***Abstract* – This paper presents a short functionality description of a Forward converter with active clamping of the voltage across the transformer and with complete rectification of the secondary side voltage. The main subject is the determination procedure to obtain a linear model of the converter, avoiding its small-signal characterization. The intention is to control the output current by acting on the duty cycle of switches S_1 and S_2. The theoretical results will be compared with numerical simulation results of the converter. A 550W prototype is built in order to verify an appropriated control loop.**

I. INTRODUCTION

The Forward converter with active clamping (FAC) is a topology that uses two active switches, operating in a complementary way, making feasible the soft commutation of them. The topology, shown in Fig. 1, has a resonant circuit during the commutation stages, which is formed by the inductance L_r and the capacitances C_{p1} and C_{p2}. The isolation and the desired level of the output voltage are obtained through the transformer T_1, which has a magnetizing inductance L_m. The output circuit configuration applies voltage through the filter formed by L_o and C_o during the conduction of the main switch S_1, as during the conduction of the clamping switch S_2. The switch S_2, when activated, gives a path for the transformer demagnetization, applying the voltage of capacitor C_1 across the primary winding.

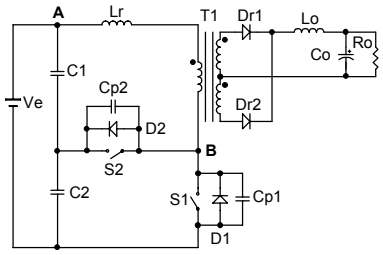

Fig. 1. Forward with Active Clamping Topology

The method used to obtain the linear circuit is based on the Vorpèrian's PWM switch model, described in [1] with the addiction of other linear elements. These elements are originated from the previous knowledge of the dynamic behavior of the converter, obtained from numerical simulations.

Applying this steps and doing the analysis of the equivalent circuit, it is determined the transfer function which describes the behavior of an output variable when applying a perturbation in one of the input variables. In this case, the objective is to analyze the dynamic response of the output current I_o, with the converter operating in continuous conduction mode, when small amplitudes of different frequencies are applied on the duty cycle that controls the switch S_1.

Using the PWM switch model, it is possible to include in the transfer function more completed and detailed results, considering the non-idealities of the circuit, such as the series resistance of inductors and switches. However, the study presented on this paper considers an idealized converter, where the parasitic elements, with exception to the equivalent series resistance (ESR) of C_o, are not considered during the small-signal characterization.

The results obtained from the theoretical transfer function will be compared with simulation results, which are taken as they were close to the real converter. The final conclusion will provide a method to predict the characteristics needed to the control loop of the converter, pointing out the significant elements of the topology.

II. LINEAR CIRCUIT DETERMINATION

The Forward converter with center tapped secondary winding is described with only two main operation stages, as shown in Fig.2. It is done in order to simplify the modeling, so the resonant stages and the magnetizing and demagnetizing intervals of inductor L_r are not considered. The two main stages are the periods where energy is transferred to the output filter:

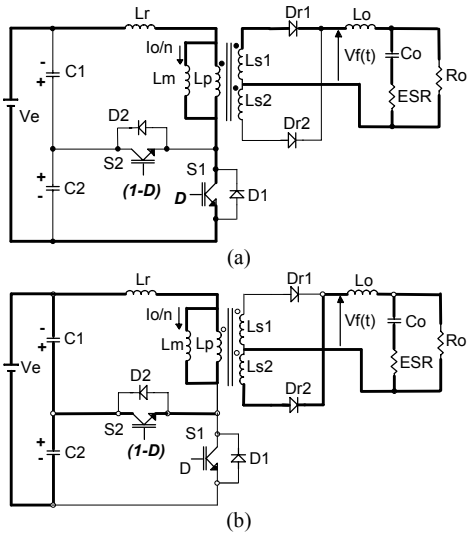

Fig. 2 – Topological stages considered to obtain the linear model
(a) 1st stage (b) 2nd stage

- *1st stage*: Switch S_1 and output rectifier D_{r1} are conducting. The voltage applied through the output filter is the input voltage V_e reflected to the secondary side;
- *2nd stage*: Switch S_2 and output rectifier D_{r2} are conducting. The voltage applied through the filter is the clamping voltage (from the capacitor C_1) reflected to the secondary side.

By doing this simplification, the voltage across the output filter ($V_f(t)$) can be represented by two voltage levels as shown in Fig.3. The switching period is represented by T_s, and the frequency by f_s.

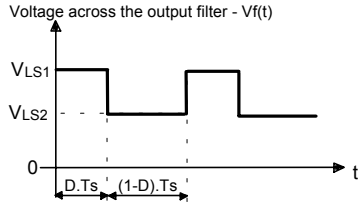

Fig. 3 –Voltage behavior across the output filter formed by L_o and C_o

The levels V_{LS1} and V_{LS2} are given in (1) and (2). Note that it is considered the transformation relation n and the losses on the static gain due to the voltage drop across the inductance L_r, represented by γ, expressed in (3).

$$V_{LS1} = \frac{V_e \cdot \gamma}{n} \tag{1}$$

$$V_{LS2} = \frac{V_e \cdot \gamma}{n} \cdot \frac{D}{D'} \tag{2}$$

$$\gamma = 1 - \frac{L_r}{L_m} \tag{3}$$

It is verified that the two voltage levels are independent. This permits the converter analysis as it is composed of two circuits, as presented by [2]. Each circuit is represented by a Buck converter, where the control of one is complementary to the other one, as Fig.4 shows.

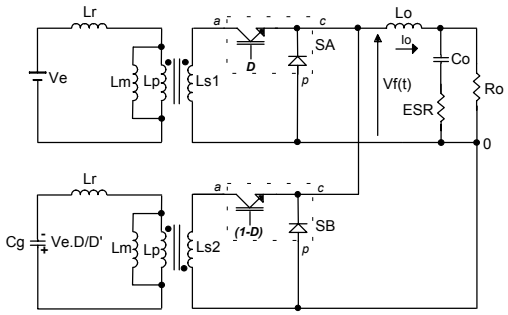

Fig. 4 – Equivalent circuit composed of two Buck converters

The static gain of each converter of Fig.4 corresponds to half of the total static gain of the Forward converter. This can be understood if the natural equilibrium of the magnetic flux of the transformer is respected.

After applying the PWM switch model to the circuit of Fig.4, the determination of the transfer function can be initiated. Considering that the input voltage V_e does not have any fluctuations, it is taken out of the linear circuit. However, this action cannot be made to the circuit that represents the second stage, once that the dynamic behavior of the equivalent clamping capacitor C_g is of interest.

$$C_g = C_1 + C_2 \tag{4}$$

If this dynamic was not considered, the resulting transfer function would be identical to a Buck converter behavior, where the dynamic responses would be affected, basically, by the output filter.

Fig.5 shows the linear circuit with the continuous conduction mode PWM switch model applied. The resonant inductance L_r is reflected to the secondary side, and the voltage across C_g (clamping voltage) is represented by a source which has its value dependent of the perturbation frequency ($V_{Cg}(S)$).

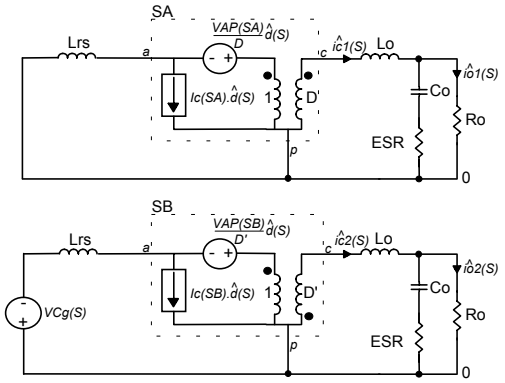

Fig. 5 – PWM switch model applied to the circuits

The values of voltage and current from the model when operating without any perturbation, are obtained after analyzing the Fig. 4:

$$V_{AP}(SA) = \frac{V_e \cdot \gamma}{n} \tag{5}$$

$$V_{AP}(SB) = \frac{V_e \cdot \gamma}{n} \cdot \frac{D}{D'} \tag{6}$$

$$I_c(SA) = I_c(SB) = I_o \tag{7}$$

As each circuit is connected to the same load, a superposition analysis can be done. By doing this, each circuit will present a distinguished behavior when a perturbation is applied to the duty cycle. The total dynamic response of the converter, $G_p(S)$, will be the sum of the two transfer functions, as shown in (8).

$$G_p(S) = \frac{\hat{io}(S)}{\hat{d}(S)} = \frac{\hat{io}1(S)}{\hat{d}(S)} + \frac{\hat{io}2(S)}{\hat{d}(S)} \tag{8}$$

The behavior of the voltage across the clamping capacitor was obtained using numerical simulations of the converter. With these simulations, it was verified that the clamping voltage follows the perturbations on the duty cycle up to a certain frequency. For frequencies close to this, it was verified a considerable attenuation of the clamping voltage oscillation. Above this frequency, the clamping voltage does not follow anymore the

perturbations on the duty cycle, and consequently, the perturbation on the output voltage and current are not existent.

Bode diagrams of gain and phase were plotted changing the perturbation frequency. This permitted the determination of a linear model that could represent the dynamic of the clamping voltage. In the Fig.6, the voltage source $V_{Cg}(S)$ is substituted by the circuit that describes this dynamics. The elements C_{gs} and L_{ms} represent the clamping capacitance and the magnetizing inductance reflected to the secondary side.

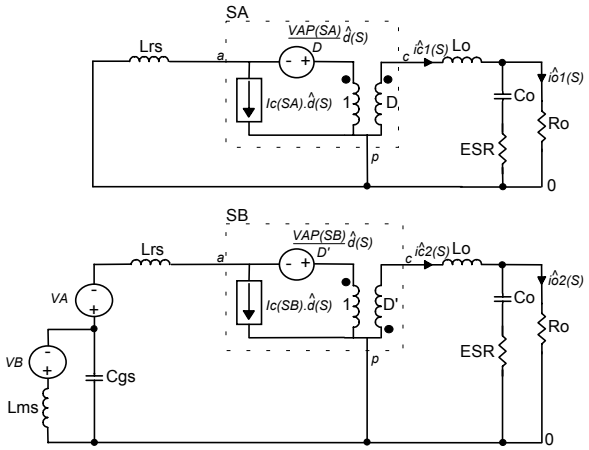

Fig. 6 – Final linear circuit to obtain the transfer function

$$L_{ms} = \frac{L_m}{n^2} \tag{9}$$

$$C_{gs} = C_g \cdot n^2 \tag{10}$$

It can be noticed that the behavior of the clamping voltage due to the perturbations on the duty cycle is related to the values of the capacitance C_g and the magnetizing inductance L_m. The voltage sources V_A and V_B are given by (11) and (12).

$$V_A = \frac{V_e \cdot \gamma}{n} \cdot \frac{D}{D'^2} \cdot \hat{d}(S) \tag{11}$$

$$V_B = \frac{V_e \cdot \gamma}{n} \cdot \frac{1}{D'} \cdot \hat{d}(S) \tag{12}$$

With the values of V_A and V_B, it is verified that the second stage circuit has a gain level equal to half of the total gain of the Forward converter, if the perturbation frequency is kept low. Increasing the perturbation frequency, this gain strongly decreases, becoming null.

By solving the linear circuit of Fig. 6, the transfer function of each circuit is obtained:

$$\frac{\hat{io1}(S)}{\hat{d}(S)} = K_1 \cdot \frac{(A_i \cdot S^2 + B_i \cdot S + 1)}{(C_i \cdot S^2 + D_i \cdot S + 1)} \tag{13}$$

$$\frac{\hat{io2}(S)}{\hat{d}(S)} = K_2 \cdot \frac{(E_i \cdot S^6 + F_i \cdot S^5 + G_i \cdot S^4 + H_i \cdot S^3 + I_i \cdot S^2 + J_i \cdot S + 1)}{(L_i \cdot S^6 + M_i \cdot S^5 + N_i \cdot S^4 + O_i \cdot S^3 + P_i \cdot S^2 + Q_i \cdot S + 1)} \tag{14}$$

The variables *Ai* to *Qi* represent expressions that consider these characteristics of the circuit: output current and voltage, capacitors C_o and C_g, inductors L_r, L_m and L_o, duty cycle D and its complement D', commutation frequency, *ESR* resistance and the transformer relation n.

$$A_i = \frac{-I_o \cdot n \cdot ESR \cdot C_o \cdot L_{rs}}{V_e \cdot \gamma} \tag{15}$$

$$B_i = ESR \cdot C_o - \frac{I_o \cdot n \cdot D \cdot L_{rs}}{V_e \cdot \gamma} \tag{16}$$

$$C_i = \left(1 + \frac{ESR}{R_o}\right) \cdot C_o \cdot \left(L_o + D^2 \cdot L_{rs}\right) \tag{17}$$

$$D_i = ESR \cdot C_o + \frac{\left(L_o + D^2 \cdot L_{rs}\right)}{R_o} \tag{18}$$

$$E_i = \frac{I_o \cdot n \cdot D' \cdot ESR \cdot C_o \cdot L_{rs} \cdot \left(L_{ms} \cdot C_{gs}\right)^2}{V_e \cdot \gamma} \tag{19}$$

$$F_i = \frac{I_o \cdot n \cdot D' \cdot L_{rs} \cdot \left(L_{ms} \cdot C_{gs}\right)^2}{V_e \cdot \gamma} \tag{20}$$

$$G_i = \frac{I_o \cdot n \cdot D' \cdot ESR \cdot C_o \cdot L_{ms} \cdot C_{gs} \cdot \left(2 \cdot L_{rs} - L_{ms}\right)}{V_e \cdot \gamma} \tag{21}$$

$$H_i = L_{ms} \cdot C_{gs} \cdot \left[ESR \cdot C_o + \frac{I_o \cdot n \cdot D' \cdot \left(2 \cdot L_{rs} - L_{ms}\right)}{V_e \cdot \gamma}\right] \tag{22}$$

$$I_i = L_{ms} \cdot C_{gs} + \frac{I_o \cdot n \cdot D' \cdot ESR \cdot C_o \cdot \left(L_{rs} - L_{ms}\right)}{V_e \cdot \gamma} \tag{23}$$

$$J_i = ESR \cdot C_o + \frac{I_o \cdot n \cdot D' \cdot \left(L_{rs} - L_{ms}\right)}{V_e \cdot \gamma} \tag{24}$$

$$L_i = \frac{\left(R_o + ESR\right) \cdot C_o \cdot \left(L_{ms} \cdot C_{gs}\right)^2 \cdot \left(L_o + D' \cdot L_{rs}\right)}{R_o} \tag{25}$$

$$M_i = \left(L_{ms} \cdot C_{gs}\right)^2 \cdot \left(ESR \cdot C_o + \frac{L_o + D' \cdot L_{rs}}{R_o}\right) \tag{26}$$

$$N_i = L_{ms} \cdot C_{gs} \cdot \left[L_{ms} \cdot C_{gs} + \frac{\left(R_o + ESR\right) \cdot C_o \cdot \left(2 \cdot L_o + D' \cdot \left(2 \cdot L_{rs} - L_{ms}\right)\right)}{R_o}\right] \tag{27}$$

$$O_i = L_{ms} \cdot C_{gs} \cdot \left[2 \cdot ESR \cdot C_o + \frac{2 \cdot L_o + D' \cdot \left(2 \cdot L_{rs} - L_{ms}\right)}{R_o}\right] \tag{28}$$

$$P_i = 2 \cdot L_{ms} \cdot C_{gs} + \frac{\left(R_o + ESR\right) \cdot C_o \cdot \left(L_o + D' \cdot \left(L_{rs} - L_{ms}\right)\right)}{R_o} \tag{29}$$

$$Q_i = ESR \cdot C_o + \frac{L_o + D' \cdot \left(L_{rs} - L_{ms}\right)}{R_o} \tag{30}$$

The values K_1 and K_2 represent the static gain of each circuit:

$$K_1 = K_2 = \frac{V_e \cdot \gamma \cdot \delta_1}{R_o \cdot n} \quad (31)$$

Where δ_1 is the compensation on the gain due to the loss included by the intervals where the voltage across the primary winding is null. This loss is consequence from the commutation stages, involving the elements L_r, C_{p1} and C_{p2}

$$\delta_1 = 1 - \frac{2 \cdot I_o \cdot L_r \cdot f_s}{V_e \cdot n \cdot D} \quad (32)$$

III. Verification with Numerical Simulations

One idealized converter and other including additional elements will be compared with the theoretical results by plotting the Bode diagrams for gain and phase. The simulated circuit is shown in Fig.7.

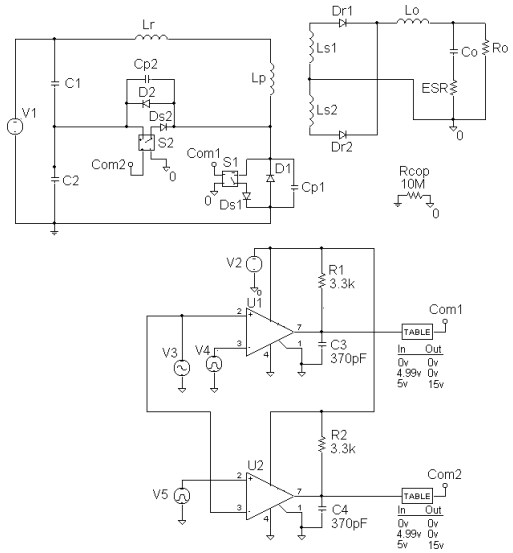

Fig. 7 – Simulated circuit to verify the Forward converter dynamic

The perturbation on the duty cycle used on the simulations is represented by a sinusoidal signal. It must be noticed that that transfer function has poles and zeroes dependent of the duty cycle D. So, the amplitude of the perturbations is limited to 1 up to 5% of the nominal duty cycle. The simulation results are expressed as the amplitude of the perturbation on the output current, considering the phase difference to the signal applied in the duty cycle.

In the first case, it is denominated an idealized converter that one where the switches resistance are disregarded ($1m\Omega$), the diodes are ideals and the elements necessary to the soft commutation (L_r, C_{p1} e C_{p2}) are not in the circuit. The ESR of capacitor C_o is considered.

Specifications of the simulated converter:

Input voltage: $V_e = 415V$
Output current: $I_o = 13,1A$
Output voltage: $V_o = 42V$
Switching frequency: $f_s = 40kHz$
Transformer magnetizing inductance: $L_m = 1,4mH$
Transformer relation: $n = 5,67$
Clamping capacitance: $C_1 = C_2 = 2,2\mu F$
Output filter inductance: $L_o = 339\mu H$
Output filter capacitance: $C_o = 220\mu F$
ESR of capacitor C_o: $ESR = 60m\Omega$

Fig.8 and Fig.9 illustrate the theoretical and simulation results:

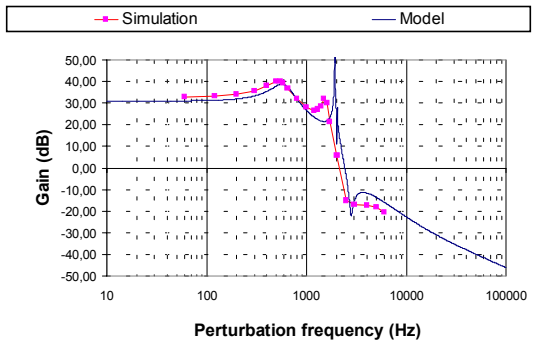

Fig.8 – Simulation and theoretical results – Gain.

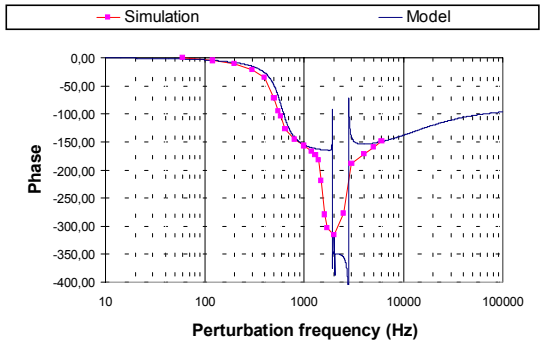

Fig.9 – Simulation and theoretical results – Phase.

In the second case, the simulations were done adding the capacitors C_{p1} and C_{p2}, and the resonant inductance L_r. It is used real models for the diodes D_1 and D_2 (MUR490) and the conduction resistances of S_1 and S_2 are equal to 1Ω.

Resonant capacitance: $C_{p1} = C_{p2} = 420pF$
Resonant inductance: $L_r = 109\mu H$

Fig.10 and Fig.11 illustrate the theoretical and simulation results:

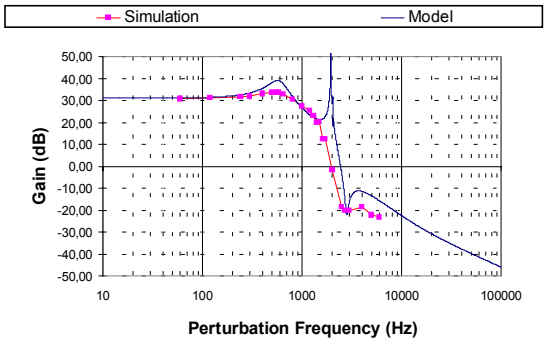

Fig.10 – Simulation and theoretical results – Gain.

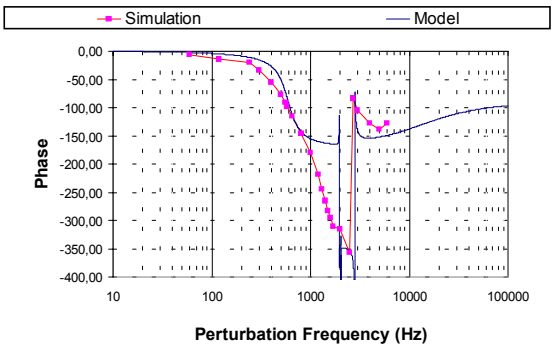

Fig.11 – Simulation and theoretical results – Phase.

IV. Experimental Results

A 550W prototype was build to verify the static characteristics of the converter. This prototype is mentioned to demonstrated the way the converter was controlled.

Fig. 12 shows the control diagram applied in the prototype. The current loop is the fastest, and uses the transfer function determined in this paper. A voltage loop is also present, but its dynamic is much slower than the current loop.

Fig. 13 is the Bode diagram of the gain obtained for the prototype, applying the transfer function expressed in (8). Fig. 14 shows the phase behavior.

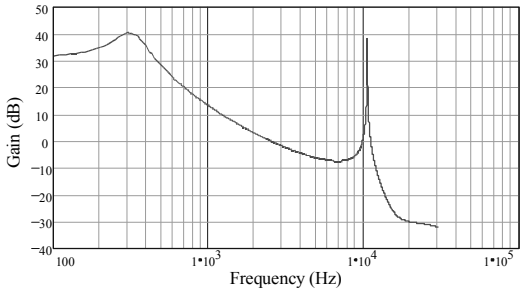

Fig.13 – Prototype Transfer function Gp(S) - Gain

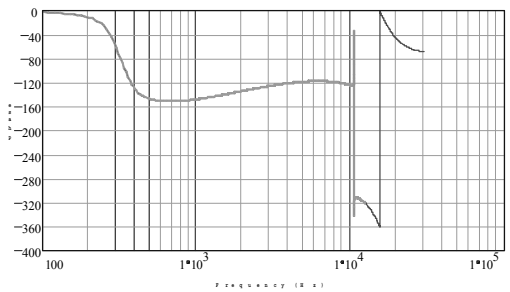

Fig.14 – Prototype Transfer function Gp(S) - Phase

The employed control was adjusted in order to avoid instabilities originated from the clamping circuit elements. A PID controller was used, with the crossover frequency of the open loop adjusted in a value lower than the frequency where phase abruptly changes. The controller applied to the prototype is shown in Fig.15.

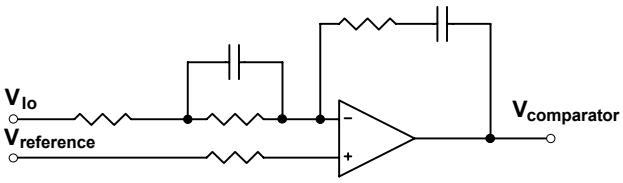

Fig. 15 – Current loop controller

With a low crossover frequency, the poles and zeroes of the controller are adjusted, regarding only to the characteristics of the output filter:

- A pole in the same frequency of the zero originated from the ESR of C_o;
- A pair of zeroes in the same frequency of the complex poles originated from the output filter C_o and L_o.

Fig. 16 is the Bode diagram of the gain obtained from the open current control loop. Fig. 17 shows the phase. It can be noticed that the instability is avoided with the right choose of the crossover frequency.

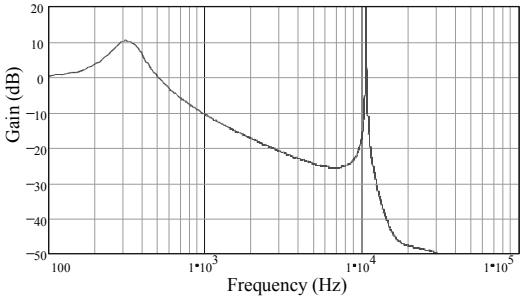

Fig.16 – Open current control loop - Gain

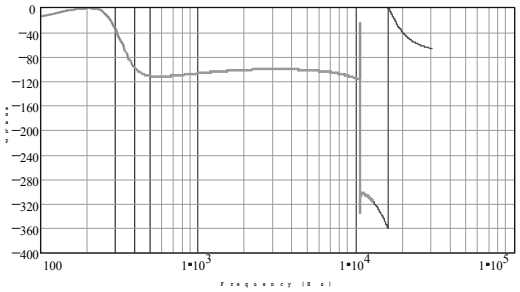

Fig.17 – Open current control loop - Phase

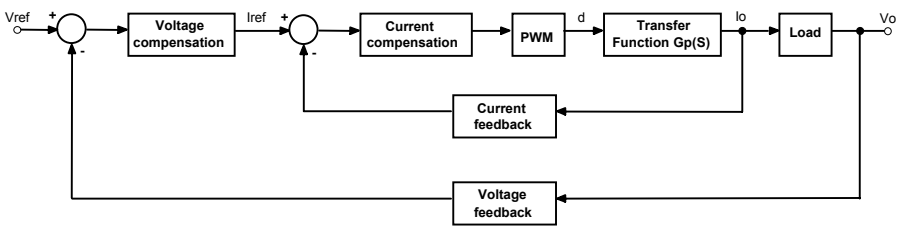

Fig.12 – Control method used in the prototype

An efficiency of 91% was obtained with the prototype at 550W, when operating with a switching frequency of 40kHz, input and output voltages of 400V and 48V respectively. Keeping a slow control speed, the instabilities originated from the 136nF clamping capacitance and the 1.27mH magnetizing inductance where not present for small perturbations on the load.

Some waveforms from the prototype are shown to illustrate the static behavior of the converter. Fig.18 illustrates the current and voltage through the primary winding, where can be noticed the intervals with null voltage. Fig.19 and Fig.20 show the current and voltage stress through the switches S_1 and S_2.

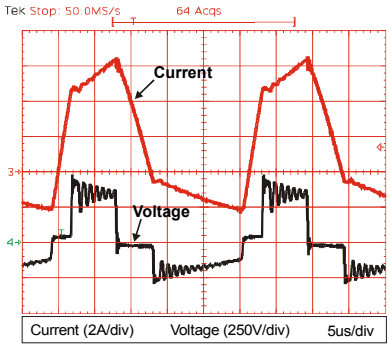

Fig.18 – Current and voltage across the primary winding

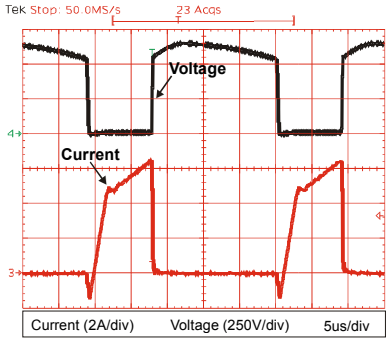

Fig.19 – Voltage and current in S_1

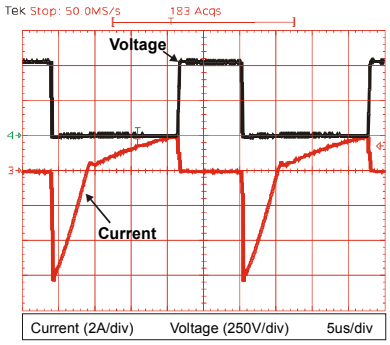

Fig.20 – Voltage and current in S_2

V. Conclusion

It was shown in this digest, the methodology employed to determine the transfer function of a Forward converter with active clamping and complete rectification of the secondary voltage. The final expression describes the behavior of the output current when a perturbation is applied to the control duty cycle.

The transfer function of this converter, even being algebraically complex, can be resumed in a simplified way having the following singularities:

- One high frequency zero (higher value than the switching frequency) set by the resonant inductance;
- One zero set by the equivalent series resistance of the output capacitor C_o ;
- Two complex poles given by the output filter;
- Two complex poles in a frequency right beneath the resonance of the clamping capacitance and the magnetizing inductance;
- Two complex zeroes in a frequency right above the resonance of the clamping capacitance and the magnetizing inductance.

Recent studies done by [3] and [4] consider the strong effect of the clamping circuit on the dynamics of converters with active clamping. This paper demonstrated that for this topology, the magnetizing inductance and the clamping capacitance would indicate the frequency value in which the transformer core can be demagnetized. As a consequence, the speed of the control loop will be strongly related to this aspect.

A prototype of the FAC Converter was build in order to verify its dynamic response to small perturbations in the load. The control applied was a PID controller, where the crossover frequency of the open current control loop was set below the frequencies where the clamping circuit produces instability.

VI. References

[1] V. Vorpèrian, “Simplified analysis of PWM converter using the model of the PWM switch: Part 1 – Continuous Conduction Mode”, in *VPEC Newsletter Current,* 1988.

[2] I. D. Jitaru and S. Bîrcă-Gălăteanua, “Small-signal characterization of the forward-flyback converters with active clamp”, in *APEC 98,* 1998, pp. 626-632.

[3] Y. Hakoda, T. Ninomiya, M. Shoyama, et al., “Effect of clamp capacitor on the stability of active-clamp DC-DC converters”, in *PESC98*, 1998, pp. 355-361.

[4] Q. Li, F. C. Lee and M. M. Jovanovic, “Large-signal transient analysis of forward converter with active-clamp reset”, in *PESC98,* 1998, pp. 633-639.